06 Apr 1995, 1:30 pm - 3:00 pm

Some Aspects of Liquefaction Assessment of Duncan Dam

V. S. Pillai
BC Hydro, Canada

R. A. Stewart
BC Hydro, Canada

H. D. Plewes
Klahn Crippen Ltd., Canada

Proceedings: Third International Conference on Recent Advances in Geotechnical Earthquake Engineering and Soil Dynamics, April 2-7, 1995, Volume I, St. Louis, Missouri

Some Aspects of Liquefaction Assessment of Duncan Dam

Paper No. 6.25

V.S. Pillai and R.A. Stewart
Geotechnical Department, BC Hydro, Burnaby, B.C., Canada

H.D. Plewes
Klohn Crippen Ltd., Richmond, B.C., Canada

SYNOPSIS: A comprehensive program of field, laboratory and analytical investigations was carried out to assess the potential for liquefaction of the foundation soils and seismic stability of Duncan Dam. Duncan Dam is located on Duncan River in southeastern British Columbia, Canada. The 39 m high zoned earthfill dam is founded on a thick sequence of sands, silts and gravels. The liquefaction studies were carried out in two phases between 1988 and 1992 to characterize in detail the engineering properties of the foundation soils; and to assess its potential for triggering liquefaction, and the post-liquefaction stability and deformation of the dam using parameters based on two approaches; one a site specific laboratory based "direct method" (Lab.method) and the other an "indirect method" (Seed's method) which is based on field penetration data and field experience during past earthquakes. This paper describes some advanced aspects of the field and laboratory investigations including laboratory testing of undisturbed soil samples obtained after freezing the ground insitu. The influence of confining stress (K_o) and initial static shear stress (K_α) on liquefaction were investigated and site specific correlations for K_o and K_α are presented. The laboratory investigations indicate that the residual strengths of the liquefied sand is a function of initial consolidation stress.

INTRODUCTION

Duncan Dam is located on the Duncan River approximately 8 km north of Kootenay Lake in southeastern British Columbia (Fig.1). The dam was constructed between 1965 and 1967 under the Columbia River Treaty to provide storage for flood control and hydroelectric generation in the Columbia Basin. The dam is a zoned earthfill embankment and is founded on a thick sequence of sands, silts and gravels. These sediments were deposited during the glacial and post-glacial periods in a deep canyon below the present Duncan River valley. Seepage through the pervious foundation sediments is controlled by means of an upstream blanket, a 24m deep partial slurry trench cut-off, and pressure relief wells. Figures 2 and 3 show the plan and a typical section of Duncan Dam. The layers of concern with respect to seismic stability are sand units (unit-3c) just beneath the embankment (Fig.3). Because of the loose and compressible nature of the foundation soils, the dam experienced significant settlements. Despite these large settlements, the dam has performed satisfactorily for normal loading conditions.

The present investigation concerns the liquefaction potential of the foundation soils and the performance under seismic loading. Seismic performance of the structure depends on the extent to which liquefaction is triggered, the subsequent loss of limit equilibrium stability and deformations. To determine seismic performance, one approach is to carry out dynamic effective stress analyses which includes pore pressure rise during shaking period but they are considered complex. For this reason, the conventional approach (total stress approach) and the one used by us, is to uncouple the analysis procedure as follows: (1) Triggering analysis, (2) Limit equilibrium stability using post-liquefaction

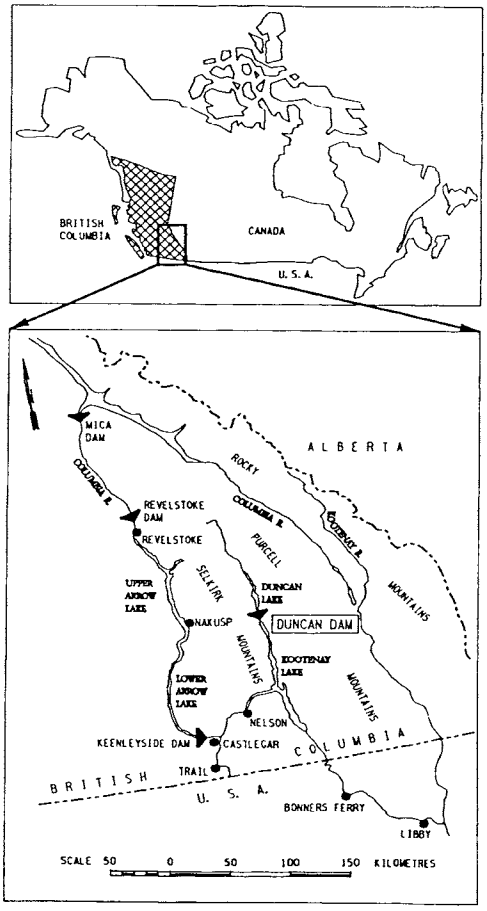

Fig.1 Location plan

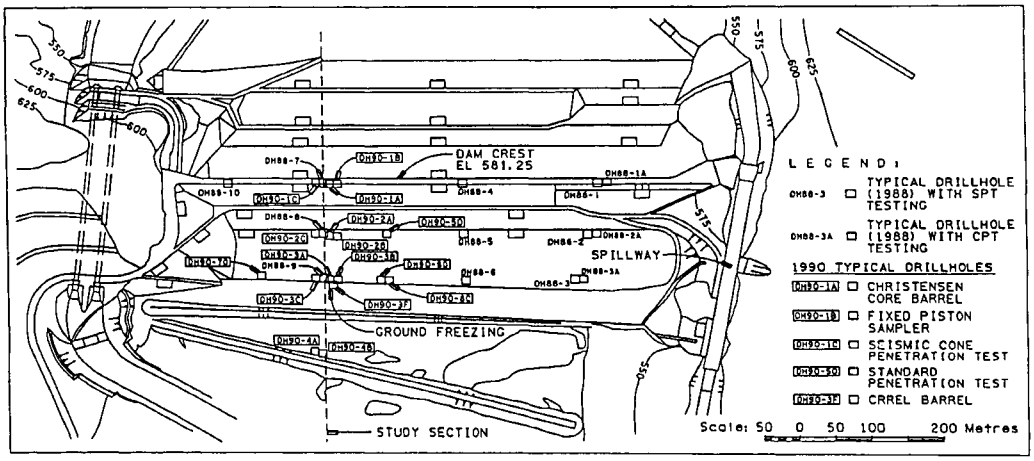

Fig.2 Field investigation plan

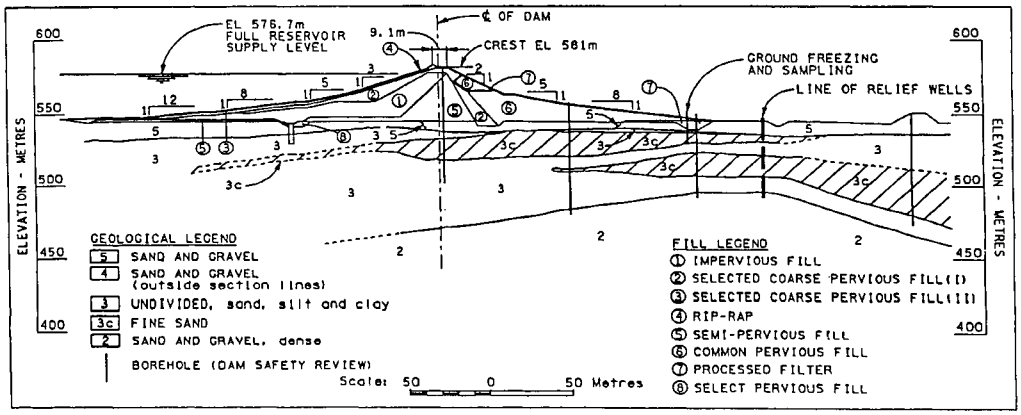

Fig.3 Typical dam section

residual strengths for the liquefied soils and (3) Deformation analysis using post-liquefaction stiffness of the liquefied soils. These analyses were carried out using two different assessment methods: namely, a site specific direct approach using soil parameters based on laboratory testing (Lab.method) and field penetration SPT-data and indirect evidence (herein described as Seed's method). Seed's method was developed by Dr.H.B.Seed and his co-workers (Seed and Idriss, 1982; Seed et.al. 1984, Seed and Harder, 1990) based on field experience during past earthquakes and field penetration data.

Under the ongoing BC Hydro Dam Safety Review, the potential for liquefaction of the foundation soils during the design earthquake and post-liquefaction stability of the dam were assessed through a comprehensive two-phased program between 1988 and 1992. The screening level Phase 1 study (1988-89) using Seed's SPT- based liquefaction assessment method (indirect approach) indicated that unit-3c sand in the right half of the dam would liquefy and lead to failure of the dam during the design earthquake (M6.5, PGA=0.12g). In view of the assumptions and empiricism involved in the indirect approach and the high cost of a potential rehabilitation of the dam, more direct site specific field and laboratory investigations of unit-3c sand were undertaken between 1990 and 1992. The objectives of the Phase 2 investigations were to obtain high quality samples of the unit-3c sand and to carry out laboratory triaxial and simple shear tests at representative confining and shear stresses to determine cyclic-liquefaction resistance and post-liquefaction residual shear strength of the sand.

This paper describes the main aspects of the field and laboratory investigations at Duncan Dam, which represent some recent advances in the characterization of liquefaction behaviour of sands. The focus of the paper, however, is on the evaluation of soil parameters such as liquefaction resistance and residual strength. The other aspects of the liquefaction assessment such as the triggering analysis and the post-liquefaction stability of the dam have been described elsewhere (Pillai and Stewart, 1994 and Pillai and Salgado, 1994).

PHASE 1- FIELD INVESTIGATION

The screening level (Phase 1) investigation comprised 10 SPT drillholes and three CPT soundings to determine the spatial distribution of the soils beneath the downstream slope of the dam and to identify the basic engineering properties

of the foundation soil units. The drillholes and CPT soundings were located along three sections through the downstream half of the dam (Fig. 2). The drillholes and soundings were extended to a maximum depth of 70 m into the foundation soils below the embankment.

Standard Penetration Tests (SPT)

The Standard Penetration Tests were carried out at 1.5 m intervals in accordance with the standard test specifications given by ASTM-1586 and the recommendations for SPT testing outlined by Seed and De Alba (1984). The drilling was carried out using mud rotary techniques using a Mayhew-1000 rig. The rod energy applied during the SPT tests was measured using an SPT energy calibrator. The energy efficiency of the donut-type hammer used was measured to be 43% .

Cone Penetration Tests (CPT)

During Phase 1, Cone Penetration Test soundings were conducted along the section of the dam to the left abutment. The CPT soundings were performed using a Fugro 15 cm^2 subtraction type electrical piez-cone. The CPT soundings provided continuous stratigraphic profiles through the foundation soils which agreed with soil information from SPT samples. More importantly, the continuous CPT data confirmed the absence of any anomalies which could have been missed by the discontinuous SPT sampling at 1.5 m intervals.

PHASE 2 - FIELD INVESTIGATIONS

The Phase 2 field investigations were carried out between May and July 1990. Soil sampling and borehole density logging were conducted at four locations along a study cross-section through the right half of the dam. Three drill sites were located on the dam; one at the dam crest (DH90-1), one about the middle of the downstream slope (DH90-2), and third at the downstream toe (DH90-3). The fourth drill site (DH90-4) was located approximately 100m beyond the toe of the dam. The locations of the drill sites are shown on Figure 2. In addition to the soil sampling during the Phase 2, three additional SPT drill holes and four seismic SCPT soundings were carried out in the right half of the dam. This work was undertaken to obtain additional $(N_1)_{60}$ measurements and to measure insitu shear wave velocities in the foundation soils.

Soil Sampling of Unfrozen Ground

At each of the four drill sites, the alluvial foundation soils were sampled to a maximum depth of 70 m below the embankment in two separate boreholes by Shelby tubes using a fixed piston sampler and by a specialized method of soil coring utilizing a Christensen core sampler with an inner PVC core liner. The tube samples were recovered at pre-selected depths. The soil coring was performed continuously with depth. Details of the soil sampling of unfrozen ground is presented by Plewes et. al. (1994).

The recovered samples of the unit-3c sand using both methods were frozen in the field in an attempt to preserve the fabric and density of the soil structure. The samples in the Shelby tubes and PVC core liner were frozen uni-directionally from the bottom upwards using dry ice and an electric freezer at the site. After freezing, observations of expelled water at the top of the samples were made and axial heave of the soil samples measured. Small axial heaves of less than 0.5 % were typically recorded for the clean unit-3c sands.

Insitu Ground Freezing and Frozen Soil Sampling

Insitu freezing of the unit-3c sand between the depths of 12 m and 17 m was conducted at location DH90-3 near the dam toe (Fig. 2) using liquid nitrogen. The frozen soil was then sampled using a 100 mm diameter CRREL (Cold Region Research Engineering Laboratory) core barrel. A total of 7.7 m of excellent quality frozen core was obtained. The details of the ground freezing and sampling are described by Sego et al. (1994) and are summarized below.

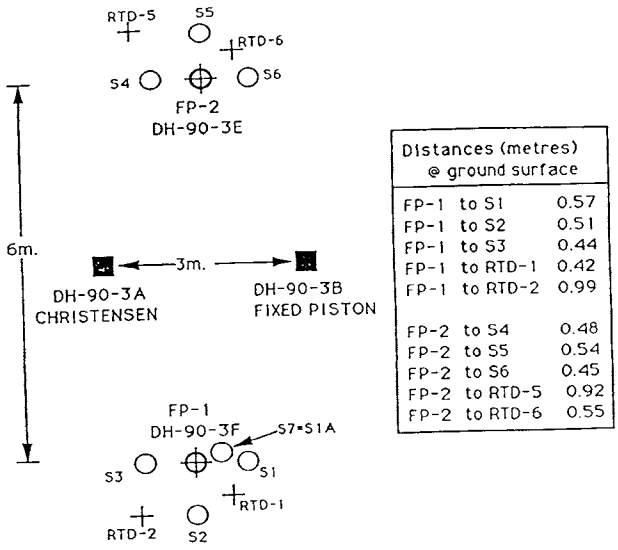

Fig.4 Ground freezing: Layout plan

Two freeze pipes, FP-1 and FP-2 were installed into the unit-3c sand layer to produce two frozen soil columns at approximately 6 m apart. The plan view of the two freeze pipes together with various sampling holes (S) and the temperature measuring probes (RTD) are shown on Fig. 4. The 50 mm diameter steel freeze pipes, FP-1 and FP-2, were installed to freeze the unit-3c sand at depth between 12m to 18m and 16m to 21m respectively. Figure 5 shows the section in detail. The tip of the freeze pipe was designed with a special hardened steel cutter (jetting pipe) which was used to advance the freeze pipe with minimum disturbance to the insitu sand. The freeze pipe system was installed through a 150 mm diameter steel casing which was previously advanced to the bottom of the embankment fill (~ 10 m). In the foundation soil (unit-3c), the freeze pipe was advanced by jetting and slow steady pushing by the drill rig. The freeze pipe sections were 7m long and were stabilized and centered within the upper casing using evenly spaced stabilization rings. The bottom of the freeze pipes were sealed using a bentonite plug. A 13 - mm diameter copper

pipe was placed in the steel freeze pipe to transfer the refrigerant to the bottom. The locations of the temperature monitoring holes were selected in order to measure the radial advance of the freezing front and are shown on Fig.4. Each hole contained one temperature measuring probe (RTD) placed at the desired depth within a 19 mm plastic tube and at a selected distance from the freeze pipe. The borehole was advanced from the surface without using a casing.

Liquid nitrogen was brought in a tanker to the site and was introduced into both freeze pipes through a piping system designed for the extreme cold freezing temperature (-190°°C). For the first 40 hours of freezing, the temperature decreased rapidly, but then the temperature drop slowed. Freezing continued for 13 days. Three tanker loads or about 60 tons (~ 68,000 L) of liquid nitrogen were used over this 13- day period. A successful frozen soil column was formed at the FP-1 and no significant frozen soil column was produced at FP-2. Frozen samples were cored using a 100 mm CRREL barrel in S1 and S1A adjacent to the freeze pipe, FP-1. A total frozen core length of 3.4 m in S1 and 4.3 m in S1A were recovered. Following a series of protocols to preserve the frozen samples, the samples were transported by a truck equipped with freezers to a cold storage facility for subsequent testing in Vancouver.

Borehole Density Logging

The density of the insitu soils was determined by borehole density logging following completion of the soil sampling work. The principal logging tool was a compensated gamma-gamma (nuclear) density tool which was used to quantitatively measure the insitu bulk soil density. The boreholes were also logged with a neutron-porosity tool to qualitatively assess variations in soil water content. Details of the borehole density logging, void ratio analysis and interpretation are described in Plewes et.al. (1994).

A minimum of three logging runs using the tool was carried out in each borehole to assess the repeatability of the tool measurements. The log was recorded in ASCII format onto computer diskettes. Using the tool readings, the void ratio profiles of the soil were determined based on Plewes et al. (1988). Typical void ratio profiles of the insitu foundation soils are shown on Fig. 6. The high repeatability of the density tool is demonstrated by the narrow envelope of the void ratio profiles. The variation in the void ratios among repeated logging runs is typically generally less than 0.03.

The insitu void ratios calculated from the density log data were compared with insitu void ratios measured from the high quality soil samples obtained by insitu ground freezing to evaluate the

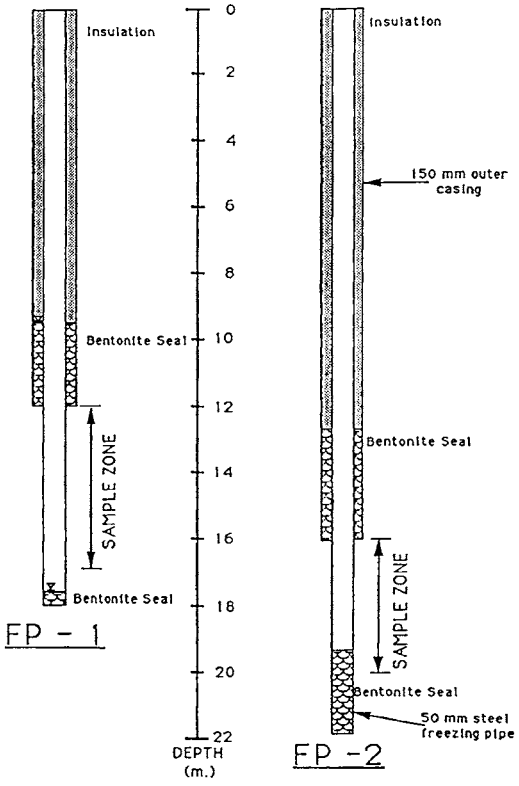

Fig.5 Ground freezing: Section of freeze pipes

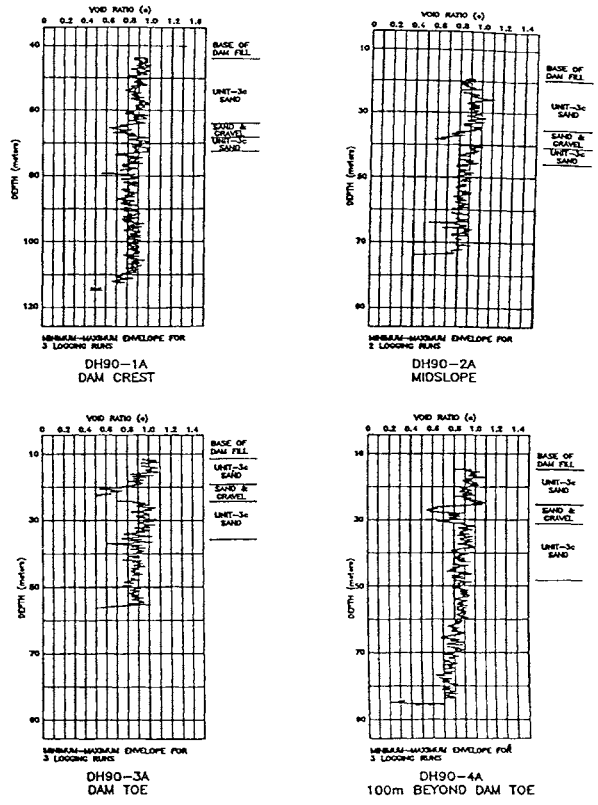

Fig.6 Nuclear density log void ratio profiles in the foundation soils beneath Duncan Dam

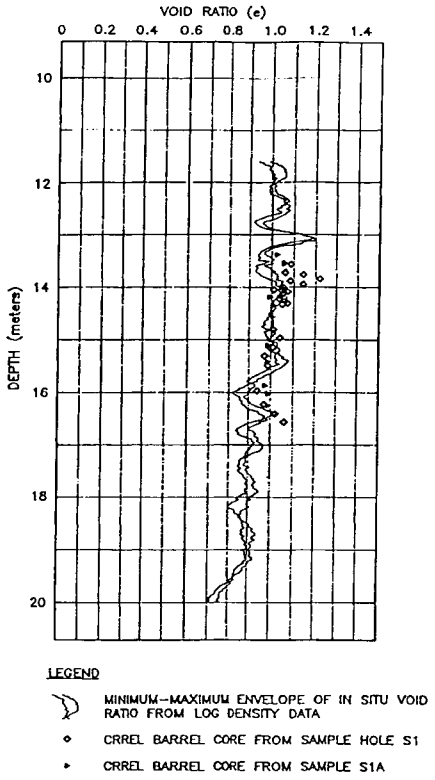

Fig.7 Comparison of nuclear density log void ratio profiles with void ratios of in situ frozen unit-3c sand samples

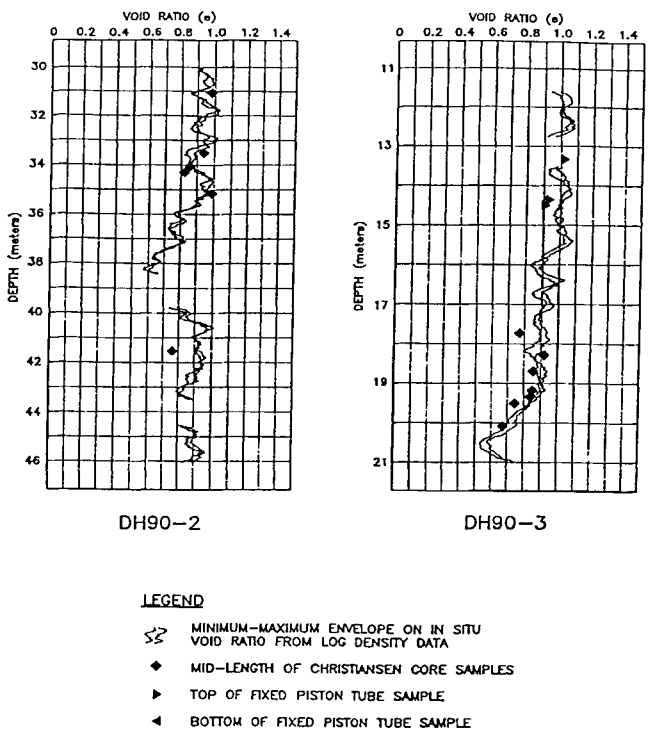

Fig.8 Comparison of nuclear density log void ratio profiles with estimated in situ void ratios of fixed piston and Christensen core samples

accuracy of the borehole void ratio profiles and assess the quality of the soil samples for laboratory testing. Figure 7 compares the void ratios interpreted from the borehole density logging and the insitu frozen soil samples. Overall, the borehole void ratio profiles correlated very well with the void ratios of the insitu frozen soil samples. The majority of the void ratios for the insitu frozen soil samples lie slightly above borehole void ratio profiles, with an average difference in void ratio of only 0.02. Figure 8 compares the void ratios of the piston tube and core samples with the interpreted density log void ratio profiles, respectively. The specimen void ratios were almost equally distributed above and below the borehole void ratio profiles. Importantly, the specimen void ratios were sensitive to insitu void ratio trends, particularly between 18 m and 21 m in DH90-3. Overall, the average difference in void ratios was -0.03 indicating that the sample increased slightly in density during the sampling.

LABORATORY INVESTIGATION

The main objectives of the laboratory testing were to determine liquefaction resistance of undisturbed sand samples and residual strength of the liquefied sand under various conditions of confining stress, initial static shear and loading modes (stress-paths). One important focus was on assessing the influence of confining stresses and initial static shear on cyclic strength (liquefaction resistance) and post-cyclic response and residual strength.

Laboratory testing consisted of undrained triaxial and constant volume simple shear tests under monotonic and cyclic loadings and were carried out at the Soil Mechanics Laboratory of the University of British Columbia (UBC). Except for a few triaxial tests, the majority of the testing was performed on undisturbed soil (CRREL barrel samples), obtained from the frozen ground.

The laboratory test program was extensive and included: (1) Undrained monotonic/cyclic simple shear tests, (2) Undrained monotonic/cyclic triaxial tests in compression and extension (3) Consolidation tests (4) Index tests, such as moisture content, grain size, and max/min densities.

Physical Properties of Foundation Soil (Unit-3c Sand)

The unit-3c sand is pervasive under the downstream right half of the dam and consists of uniform fine sand (D_{50} ~ 0.2 mm) with about 5 % to 8 % fines. Representative gradation curves of the unit-3c sand are shown on Fig. 9. The sands consist of quartz, plagioclase, K-feldspar and calcite-dolomite. The grains are angular to subangular (roundness of 0.1 and 0.3) and have equant shape (sphericities of 0.7 and 0.9). The specific gravity is 2.77. The measured maximum void ratio was 1.15 and the minimum void ratio was 0.76.

Towards the left half of the dam, the foundation soils become finer and are classified as unit-3a (silty sand and sandy silt) and unit-3b (clayey silt). Phase 1 studies indicated that these soils in the left half of the dam were more resistant to earthquake liquefaction. Consequently, the focus of the Phase 2 studies

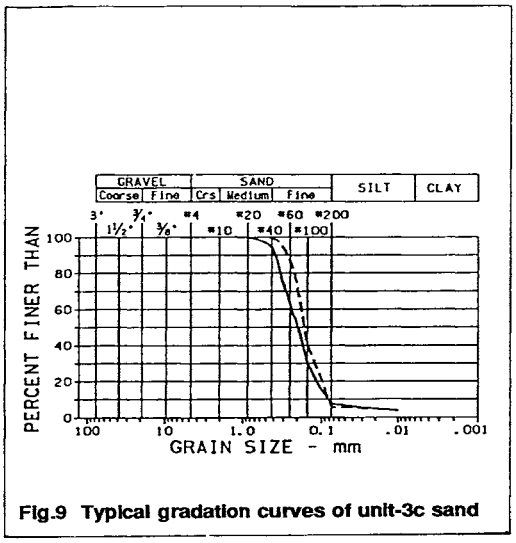

Fig.9 Typical gradation curves of unit-3c sand

were on unit-3c sand beneath the right half of the dam (Fig.3).

Shear Properties of Foundation Soil (Unit-3c Sand)

Simple shear tests consisted of both monotonic and cyclic tests on undisturbed CRREL barrel samples which were obtained from the insitu frozen ground. Both types of tests were performed with and without static shear stress. Following the cyclic loading phase, the specimens were either loaded monotonically for assessment of post-cyclic shear response of the liquefied sand, or consolidated to stresses prior to cyclic loading in order to assess post-cyclic settlements resulting from excess pore pressure dissipation. As the Duncan Dam slopes are reasonably flat (Fig.3) and the predominant loading mode in the foundation soils is in simple shear, the key parameters for the triggering and post-cyclic performance analysis (Pillai and Salgado, 1994) were derived from the simple shear tests.

Triaxial tests were carried out on undisturbed CRREL barrel samples, Christensen and Fixed piston samples. Both monotonic and cyclic tests with or without initial static shear were carried out on the undisturbed samples. As for simple shear tests, the cyclic loading phase of the triaxial tests was followed by post-cyclic monotonic loading. Monotonic shearing , pre-cyclic or post-cyclic, was performed either in compression or extension mode of loading. Details of laboratory testing are described in Pillai and Stewart (1994).

LIQUEFACTION RESISTANCE AND POST-LIQUEFACTION PARAMETERS BASED ON LAB. METHOD

Cyclic Resistance Ratio

Liquefaction resistance of soil is determined in terms of cyclic resistance ratio [CRR = τ_{cyc}/σ_c'] of the soil, which is defined as the ratio of cyclic shear stress required to trigger liquefaction to the initial normal effective stress.

Liquefaction resistance of a soil element at depth in sloping ground is given by:

[1] $CRR_\sigma = CRR_1 \cdot K_\sigma \cdot K_\alpha$

where: CRR_σ is the liquefaction resistance or the cyclic resistance ratio at an effective confining stress of σ_c'. CRR_1 is the liquefaction resistance or the cyclic resistance ratio at a confining stress, σ' = 1 tsf (~100 kpa). K_σ is a correction factor that depicts the influence of confining stress (depth), σ_c', on CRR. K_α is a correction factor that depicts the influence of initial static shear stress on the horizontal plane, $\alpha = \tau_0/\sigma_0'$, (sloping ground) on CRR.

The CRR herein is defined as the cyclic stress ratio that is required to produce 2.5 % axial strain (triaxial) in a single amplitude in 10 cycles. In cyclic simple shear tests, the equivalent shear strain is 3.75% and this was rounded off to 4% as the triggering strain.

Influence of Confining Stress on Liquefaction Resistance and K_σ-Factor

Cyclic simple shear tests and cyclic triaxial tests were carried out on undisturbed unit-3c sand samples at various confining stresses with no initial static shear stress. That is, in the triaxial tests the sample was consolidated isotropically to the predetermined effective confining stress and then cyclic loading was applied. Similarly in the simple shear tests, the samples were consolidated to the predetermined effective vertical confining stress and no horizontal shear stress applied before cyclic loading. In each test, a preset cyclic stress ratio was applied and the corresponding number of cycles that produced the triggering strain was determined. The cyclic stress ratio, CRR_σ, to trigger liquefaction in 10 cycles was determined at effective confining stresses of 200, 400, 600 and 1200 kPa.

The results show that the CRR_σ determined directly at various confining stresses is independent of the confining stress in both triaxial and simple shear loading. The CRR_σ has a value of about 0.14 in simple shear loading and 0.17 in triaxial loading (Fig.10). The value of CRR_σ in simple shear is less than that in the triaxial. The higher CRR in triaxial loading is possibly due to the difference in the initial state of soil after consolidation and prior to cycling. In the simple shear tests, the initial consolidation was along the K_o - line ($K_c = K_o$) whereas in the triaxial it was along the isotropic line or K_c = 1.0.

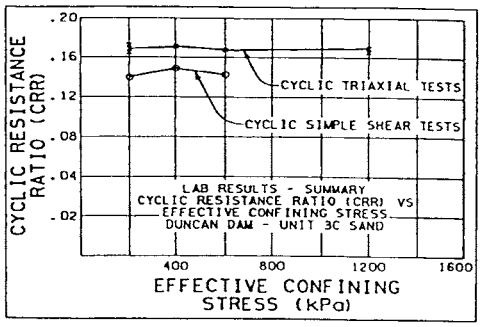

Fig.10 Lab. CRR-values (CRR_σ) versus effective confining stress, σ_c'

TABLE 1

DUNCAN DAM SAND: BACK-CALCULATED K_σ - VALUES

σ_c' (kPa)	100	200	300	400	600	800	1000	1200
$(N_1)_{60}$	10	11	12.4	13.2	14.5	15.7	17.3	18.5
$(CRR)_\sigma$	0.12	0.12	0.12	0.12	0.12	0.12	0.12	0.12
$(CRR)_1$	0.12	0.13	0.15	0.16	0.17	0.18	0.21	0.22
K_σ	1.00	0.92	0.80	0.75	0.70	0.67	0.57	0.54

As the liquefaction resistance or CRR_σ is essentially independent of confining stresses, no correction factor for the confining stresses (depth) was used for the Lab. method. Since the CRR_σ was measured in the lab, which remained constant with increased confining stresses or depth, therefore the factor, K_σ (= CRR_σ / CRR_1) could be back calculated. The CRR_1 with increased confining stresses/depth was determined from Seed's chart which was based on field experience during past earthquakes for free field conditions. That is, CRR_1 could be determined using $(N_1)_{60}$ values obtained for the soil in the field. These values for the corresponding confining stresses are shown in Table 1. Combining the field and the lab behaviour, a K_σ -curve was developed for the unit-3c sand as shown in Table 1 and Fig. 11. This curve is compared with the K_σ-curve of Seed and Harder (1990) (discussed in a later section). Details of the back-analysis is presented in Pillai and Byrne (1994).

In general, CRR decreases with increased confining stress and increases with increased density. However, there is an increase in density with increased confining stress as shown on Fig. 12. Thus, there are two factors involved in the laboratory data: (1) the density increases with confining stress and this tends to increase the CRR; and (2) the increased confining stress reduces CRR. One simple interpretation of the lab test results is that, the two factors have the opposite effects for the normally consolidated sand under consideration, and the factors happen to balance one another. Alternatively, Pillai (1991) suggested that if the initial stress-history (in e - σ_c' space) relative to an ultimate reference state such as the steady state or the critical state (initial state parameter) remains the same, then the soil cycled from that state could produce the same CRR.

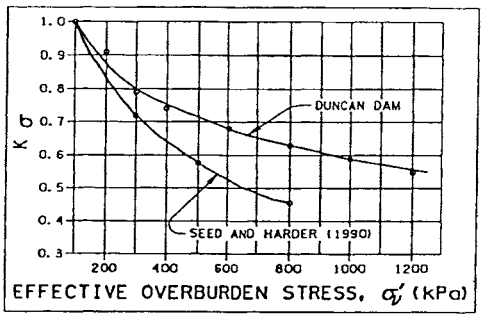

Fig.11 Duncan Dam Sand: Back-calculated K_σ - curve

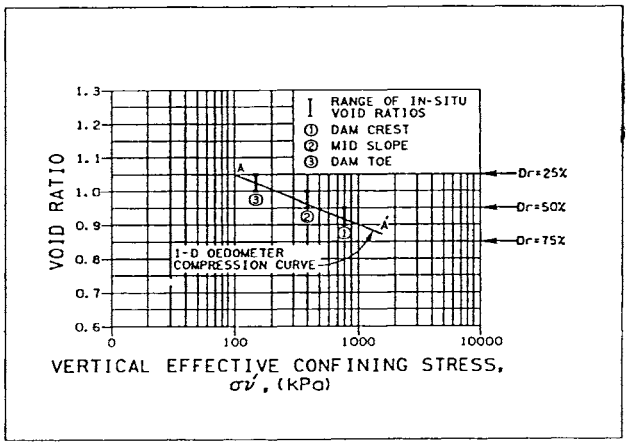

Fig.12 Lab. consolidation void ratios and measured field in situ void ratios versus vertical effective confining stress

Influence of Initial Static Shear Stress on Liquefaction and K_α Factor

Initial static shear stress (static bias) may have a significant influence on the liquefaction resistance of the soil and this influence is quantified by a correction factor K_α. The correction factor K_α is defined as the ratio of CRR at the initial static shear stress of concern to the CRR at zero static shear stress when all other factors such as initial void ratio and confining stresses are maintained the same. The factor α is defined as the ratio of shear stress on the horizontal plane to the effective normal stress. K_α varies with α. Published correlations are considered empirical and show a wide variation of K_α with α values and relative densities (Seed and Harder, 1990). For the Duncan Dam unit-3c sand, the correlation between K_α and α was determined by direct laboratory testing on undisturbed samples obtained from ground frozen insitu.

A series of cyclic simple shear tests were performed on the undisturbed sand samples consolidated to an effective confining stress of 200 kPa, and applied with initial static shear stress ratio(s), α, of 0.08, 0.16, and 0.24. The results are shown on Fig.13 and the K_α versus α plot on Fig.14 . The observed pore pressure response in cyclic simple shear tests for various initial static bias conditions is shown on Fig.15. In cyclic triaxial compression and extension tests, an initial static shear of 0.16 was introduced through anisotropic consolidation at

effective confining stresses of 200 kPa and 1200 kPa and the corresponding variations of K_α with α are shown on Fig. 14 . Typical results of cyclic stress ratio (CSR) versus number of cycles (N) in triaxial compression, extension and isotropic loading modes are shown on Fig.15 . For the cyclic simple shear conditions, CRR or K_α decreased with increasing α as shown on Figs. 13 and 14. A similar decreasing trend was observed during the cyclic triaxial extension tests (Figs. 14 and 16). However, a significant increase of CRR or K_α was observed during the cyclic triaxial compression tests (Figs. 14 and 16) .

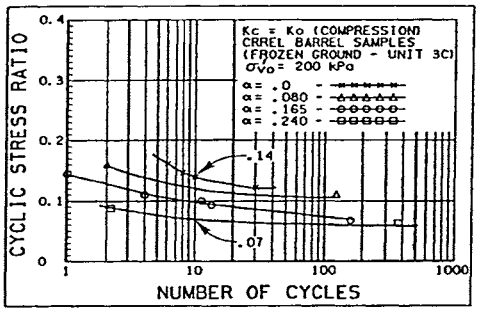

Fig.13 Cyclic simple shear test results with initial static bias, α: Cyclic stress ratio versus number of cycles

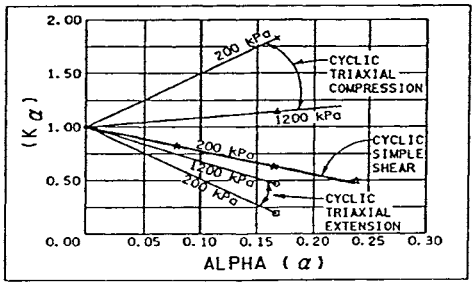

Fig.14 Variation of K_α with α for different loading modes

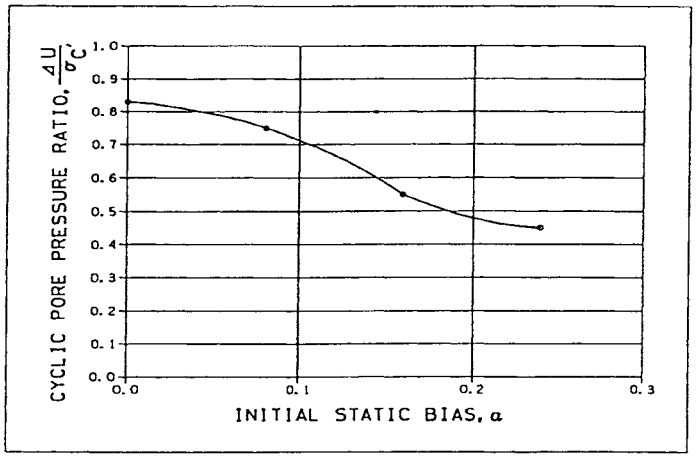

Fig.15 Cyclic simple shear test results: Pore pressure response with initial static bias, α

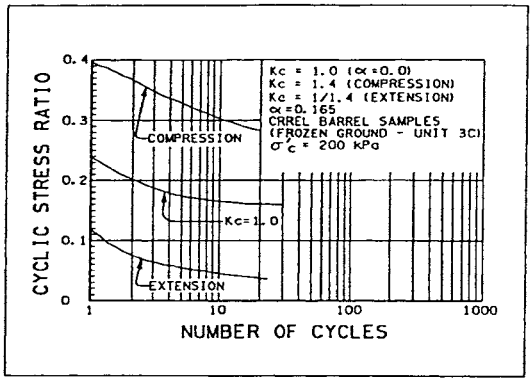

Fig.16 Cyclic triaxial test results: Compression, extension (α=0.16) and isotropic (α=0) loading modes: Cyclic stress ratio versus number of cycles

This contrasting behaviour was possibly due to the fact that the soil under consideration behaved dilatively during the triaxial compression loading while it behaved contractively during the simple shear and triaxial extension loadings, which were observed during the monotonic tests (Figs. 17 and 18). That is, the monotonic and cyclic shear behaviour of the sand were dependent on the loading mode or stress path. The predominant loading mode in the foundation soils is by simple shear. Fig. 17 shows the plot of stress-path response of four undrained monotonic simple shear tests on undisturbed sand samples. Two of these tests were consolidated to 589 kPa and 981 kPa and carried out with no initial static bias. The other two tests were consolidated to 200 kPa and applied with an initial static bias of 0.16 and 0.24. The yield surfaces (Fig. 16) illustrate the contractive behaviour of the sand during the simple shear loading mode and showing a unique "peak envelope" through the origin. The peak envelope occurs at a ϕ_u of about 19 degrees.

The stress-path response of the undisturbed unit-3c sand in undrained monotonic triaxial compression and extension tests are shown on Fig. 18. Three tests were carried out in compression with initial consolidation stress of 200 kPa, 400 kPa and 1200 kPa. Similarly, three tests in extension were carried out from the same initial consolidation stresses. The shear response was dilative in compression loading for the initial consolidation stresses of 200 kPa and 400 kPa or essentially for the same initial state as opposed to the contractive/ dilative response in the extension loading mode.

For the triggering and performance analyses of the

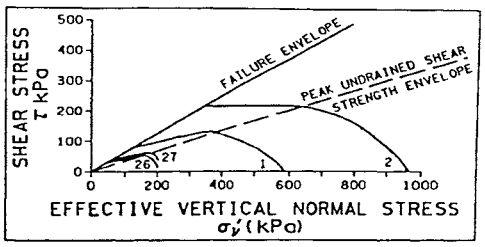

Fig.17 Undrained monotonic simple shear tests on undisturbed unit-3c sand: Stress-path response

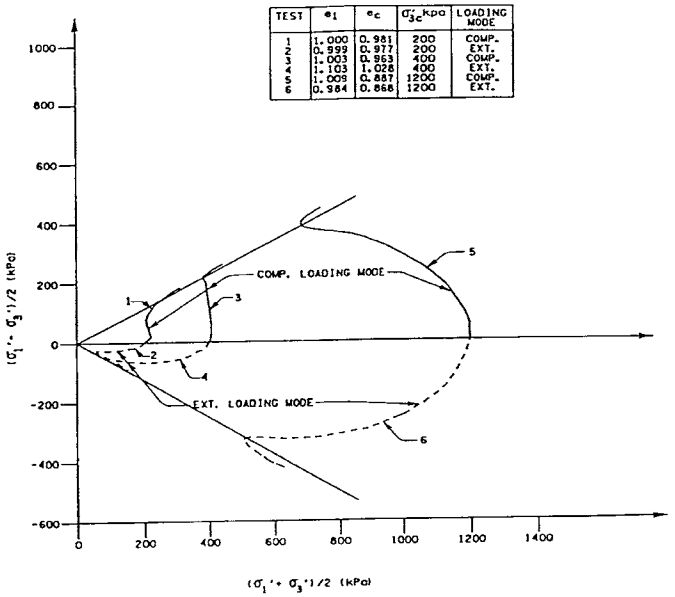

Fig.18 Undrained monotonic triaxial tests on undisturbed unit-3c sand: Stress-path plots of compression and extension loading modes

Duncan Dam, a K_α factor represented by the simple shear mode was used (Fig. 14). However, a sensitivity analysis using a K_α = 1.0 was also performed.

Undrained Shear Strength of Unit-3c Sand

The peak undrained shear strength, S_{up}, of the unliquefied zones of unit-3c sand were determined based on a series of four undrained monotonic (pre- cyclic) simple shear tests carried out on undisturbed soil samples. The simple shear monotonic tests are described previously and the results are shown on Fig. 19. Separately, to establish the undrained residual shear strength of liquefied zones of unit-3c sand, twenty three post-cyclic undrained monotonic simple shear tests were carried out. That is, after the liquefaction was triggered in a cyclic test, the soil sample was shear loaded monotonically under undrained condition to obtain a stress-strain response to a large strain level. The post-cyclic response data is subdivided into two sets as shown on Fig.20 for clarity: (1) tests carried out with the initial static bias, α=0 and (2) tests carried out with α>0. Fig.15 shows the cyclic pore pressure response at triggering determined from the undrained cyclic simple shear tests on undisturbed unit-3c sand. It indicates that there is less build-up of pore pressure ($\Delta U/\sigma_{vo}'$ = 45 %) at triggering of liquefaction when the initial static bias, α , is high as compared to a larger build-up of pore pressure of $\Delta U/\sigma_{vo}'$ = 80% when the initial static bias is low or α =0, which is a typical response of sand in contractive mode (Pillai and Stewart, 1994). The degree of pore pressure response at triggering has significant influence on the post-cyclic stress-strain response and the stiffness of the liquefied soil (Fig. 20).

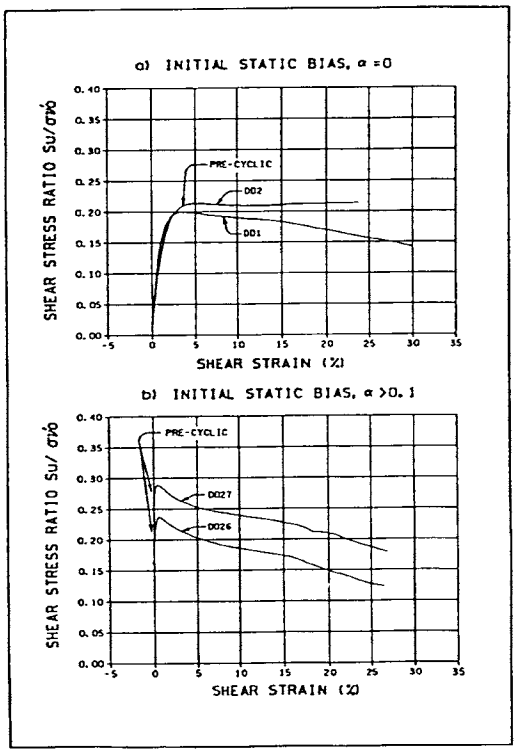

Fig.19 Undrained monotonic simple shear tests on undisturbed unit-3c sand: Stress-strain response

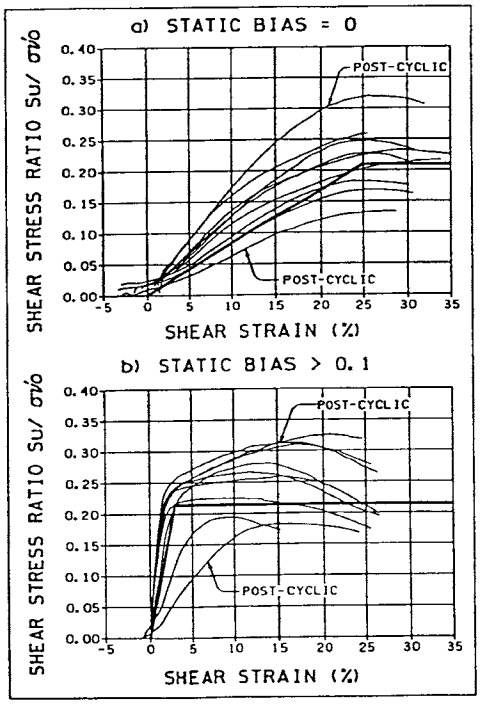

Fig.20 Post-cyclic undrained monotonic simple shear tests on liquefied unit-3c sand: Stress-strain response

Unliquefied Sand

For unliquefied sand, the peak undrained shear strength, S_{up} was used in the post-liquefaction analyses and are based on the four undrained monotonic simple shear tests on undisturbed samples. The plot of the test data is shown on Fig. 21 which indicates that the peak undrained shear strength, S_{up}, is proportional to the initial consolidation effective vertical stress, σ_{vo}', and is represented as follows:

[2] $S_{up} = 0.23\ \sigma_{vo}'$

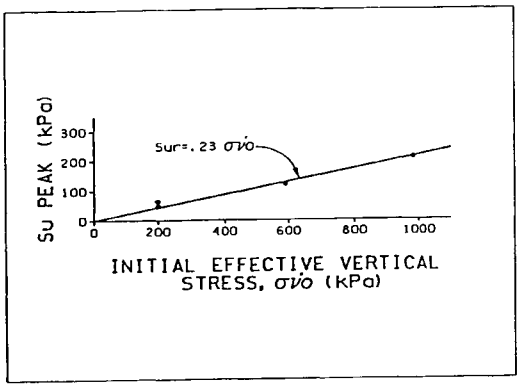

Fig.21 Undrained monotonic simple shear tests on undisturbed unit-3c sand: Plot of peak strengths with initial consolidation stress, σ_{vo}'

Liquefied Sand

The undrained residual shear strength, S_{ur} of the liquefied sand was determined based on the stress-strain results of the post-cyclic undrained monotonic simple shear tests and are shown on Fig.22. The results indicate at large strains the ratio of S_{ur}/σ_{vo}' is constant. That is, S_{ur} is proportional to the initial consolidation effective vertical stress, σ_{vo}', and is represented by:

[3] $S_{ur} = 0.21\ \sigma_{vo}$

This relationship is consistent with the critical state concepts and the concepts presented in the 1993 Rankine Lecture (Ishihara, K., 1993).

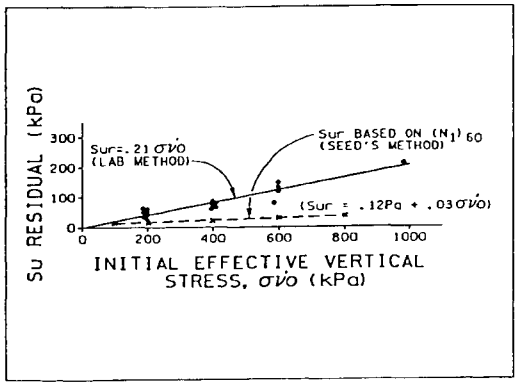

Fig.22 Undrained monotonic simple shear test on liquefied unit-3c sand: Plot of residual strengths with initial consolidation stress, σ_{vo}'

Stiffness of the Liquefied Sand

The stiffness characteristics of the liquefied sand were determined based on the same set of post-cyclic undrained monotonic simple shear test results, shown on Fig.19 . The results indicate that the stiffness modulus, G_{lim}, of the liquefied soil is about ten times larger with high initial static bias as compared to the liquefied soil with small or no static bias. As mentioned earlier, this is attributed to the fact that the pore pressure build-up at triggering was significantly less with large initial static bias as compared to that with small initial static bias.

Some Observed Shear Characteristics of Unit-3c Sand

From the laboratory testing on undisturbed unit-3c sand samples, some observed shear characteristics of interest are:

1. The soil, in general, followed a consistent initial consolidation line (ICL: A A') with increasing confining stresses (Fig.12). For any given initial consolidation stress, this line represented a consistent initial state (e_c, σ_c') for a subsequent monotonic or cyclic test.

2. Cyclic resistance ratio, CRR_q, is independent of confining stress in both triaxial and simple shear loading.

3. For the same initial stress history (e_c, σ_c'), the sand behaved differently for different stress-paths during undrained monotonic as well as cyclic loadings. That is, the material behaved dilatively during triaxial compression and contractively during triaxial extension and simple shear loading.

4. With initial static bias, α, liquefaction resistance, CRR, increased significantly for the dilative condition (triaxial compression) while it decreased for the contractive condition (simple shear and triaxial extension).

5. The residual strength, S_{ur}, of the liquefied soil is a direct function of initial confining stress. However, the stiffness of the liquefied soil appears to be dependent on the initial static bias. With high initial static bias, α , the liquefied soil is about ten times stiffer than that with low or no initial static bias.

LIQUEFACTION RESISTANCE AND POST-LIQUEFACTION PARAMETERS BASED ON SEED'S METHOD

Overburden Correction Factor, C_N and SPT $(N_1)_{60}$ Values

The right half of Duncan Dam is underlain by a deep deposit of uniform fine sand (unit-3c) with gradation as shown on Fig. 9. The field N-values increase with depth or confining stress. Despite the fact that the material is a natural deposit involving large depths and lateral distances, the N-values obtained from six drillholes lie on a relatively smooth curve with moderate scatter (Fig. 23).

Based on the energy calibration (43%) of the Mayhew drill rig, the field SPT-values , N, were corrected to 60% as follows:

[4] $N_{60} = N \cdot 43/60$

Values of the corrected SPT $(N_1)_{60}$ are related to N_{60} as follows:

[5] $(N_1)_{60} = C_N \cdot N_{60}$ [or $(N_1) = C_N \cdot N$]

where C_N is the overburden correction factor that accounts for the increased resistance due to increase in effective confining or overburden stresses and N_1 is the corrected blow count at 1 tsf (~100 kPa). In the conventional practice, $(N_1)_{60}$ can be determined with the knowledge of C_N values with depth. C_N values available in the published literature are generally limited to a maximum effective overburden stress of 6 tsf (600 kPa). At Duncan Dam, the maximum depth investigated was about 80 m from the ground surface. The foundation soil, unit-3c sand, occurs below the dam fill at about 10 m below the toe and 40 m below the crest. The overburden stress within the unit-3c sand under consideration varies from about 100 kPa (~ 1 tsf) to about 1200 kPa (~ 12 tsf).

For Duncan Dam it was possible to determine C_N values based on a back-analysis using the large pool of field and lab information that was available from the investigation. The field and lab information includes N-values and variation of relative density, D_r, with depth.

At a depth corresponding to σ_v' = 1 tsf, Fig. 23 shows N=14 and therefore N_1 = 14 since C_N =1.0 at that stress. Using this data at σ_v' = 1 tsf and the laboratory data on relative density D_r at various confining stresses, the N_1 curve was developed using the Gibbs and Holtz (1957) relationship. The values of N_1 [and $(N_1)_{60}$] were computed for various vertical effective stresses and the C_N values were determined as N_1/N The back-calculated C_N values for the Duncan Dam sand is shown by Curve-B on Fig. 24.

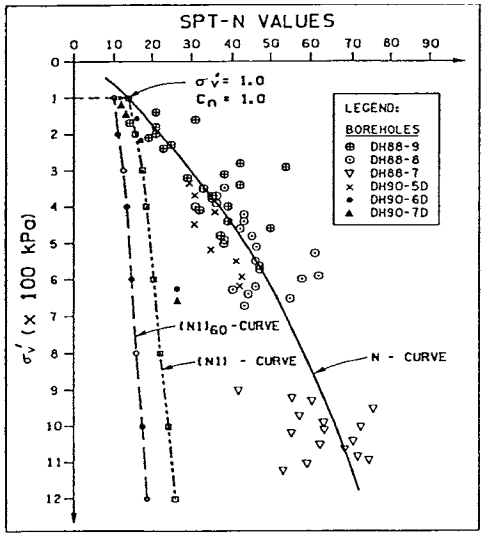

Fig.23 SPT-N and $(N_1)_{60}$ values versus effective vertical confining stresses (depth) at Duncan Dam

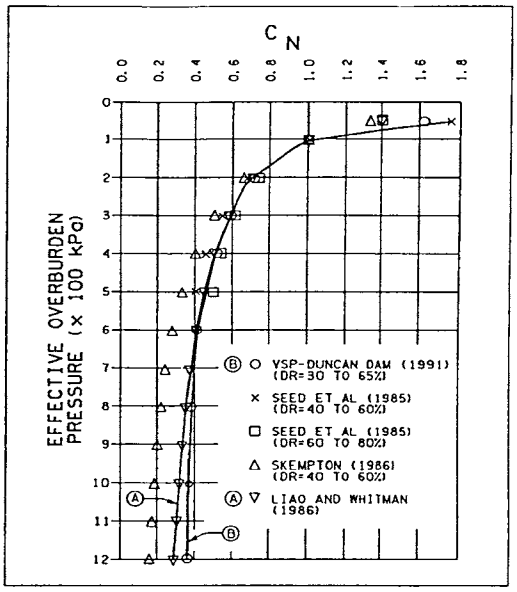

Fig.24 Duncan Dam Sand: Back-calculated C_N -curve (B)

The C_N values thus calculated are very close to those predicted by Liao and Whitman (1986) for effective vertical confining stresses of 1 to 6 tsf (D_r = 30 to 50 %). For stress levels 6 to 12 tsf (D_r= 50 to 65 %), C_N values are slightly higher than those of Liao and Whitman. The Liao-Whitman values were computed using $C_N = 1/(\sigma_v)^{0.5}$ and are shown on Fig. 24 (Curve-A).

Evaluation of CRR_1

Seed's Liquefaction Assessment Chart (Fig. 25) correlates empirically the CRR_1 with $(N_1)_{60}$ values based on past liquefaction experience. The CRR_1 represents the corrected CRR at an effective vertical confining stress of 1 tsf for level ground condition. The $(N_1)_{60}$ values at various depths were determined as described above. Seed's chart is for an earthquake magnitude of 7.5 corresponding to 15 cycles, and a correction factor of 1.17 as suggested by Seed was used to convert to a 10 cycle base and magnitude of 6.5. For a fines content of 5%, this translates to a CRR_1 value of 0.12 for $(N_1)_{60}$ of 10 at the confining stress of 1 tsf.

K_o Factor

For the SPT-based analysis (Seed's method) it is common practice to apply the K_o correction factor based on published correlations similar to Seed and Harder (1990) (Fig. 11). In this correlation, K_o decreases from unity to about 0.44 at 8 tsf (800 kPa) for medium sand. For Duncan Dam, however, the range of confining stress under consideration exceeds the range available in the published literature. Secondly, for this site, CRR_o was obtained directly from laboratory cyclic tests carried out on undisturbed samples consolidated at various confining stresses in the range of 100 kPa to 1200 kPa and CRR_o was found to be independent of confining stress. Also available are the values of $(N_1)_{60}$ at various depths or confining stresses up to about 12 tsf

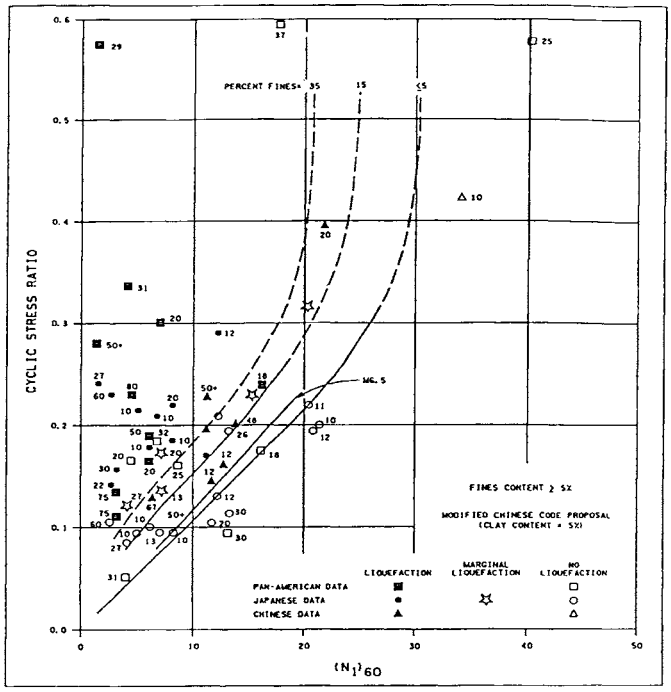

Fig.25 Relationship between stress ratios causing liquefaction and $(N_1)_{60}$ for M=7.5 earthquakes (after Seed et al., 1984)

(1200 kPa) and the corresponding CRR_1 from Seed's chart. This provided a unique opportunity to back analyze and determine the K_σ correction factor for various confining stresses up to 12 tsf (1200 kPa). The back-calculated K_σ values are shown in Table 1 and Fig. 11, which shows that the conventionally used Seed and Harder (1990) values are conservative for this sand. Pillai and Byrne (1994) provides details of the back-calculation of K_σ. They suggest that K_σ values thus obtained for Duncan Dam simulate both the increase of confining stress as well as the corresponding density increase of the soil in an actual field condition and are therefore more appropriate in estimating the actual CRR of the soil element at depth when using Seed's chart and $(N_1)_{60}$ values.

K_α Factor

For Seed's method of triggering analysis, K_α - α correlations available in the published literature (Seed and Harder, 1990) are considered empirical and they do not explicitly reflect the influence of the stress paths or initial state of the soil. These aspects were better quantified during the laboratory investigations as described under the Lab.method. Therefore the same K_α versus α relationship used for the Lab. method was applied in Seed's method of analysis.

Residual Strength of Liquefied Sand

For Seed's method, residual strength of liquefied sand was determined on Seed's chart which correlates $(N_1)_{60}$ with S_{ur} as shown on Fig. 26a (Seed and Harder, 1990). Using the SPT $(N_1)_{60}$ values shown on Fig. 26b and the average correlation curve from Seed's chart (Fig.26), the average values of S_{ur} shown on Fig.26a were obtained for the corresponding σ_{vo}'. Thus S_{ur} can be approximated by the following equation:

$$[6] \quad S_{ur} = .12\ Pa + .03\ \sigma_{vo}'$$

where Pa is the atmospheric pressure. Eq.[6] is also plotted on Fig.21 for comparison which indicates that for high confining stresses the residual strengths obtained from the Lab. method are 2 to 3 times the S_{ur} values inferred from Seed's chart. For example, at σ_{vo}' = 400 kPa, the residual strength based on the Lab. method is 84 kPa (1750 psf) as compared to 24 kPa (500 psf) based on Seed's method.

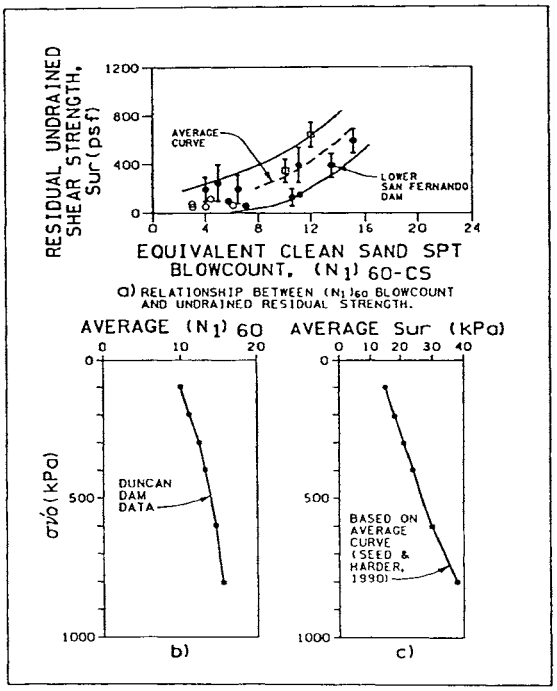

Fig.26 (a) Undrained residual shear strength, S_{ur}, versus $(N_1)_{60}$ (after Seed and Harder, 1990)
(b) σ_{vo}' versus average $(N_1)_{60}$ and
(c) σ_{vo}' versus average S_{ur} (Seed's method)

Some Aspects of Performance Analyses

Liquefaction triggering, limit equilibrium stability and deformations analyses were performed and are detailed elsewhere by Pillai and Stewart (1994) and Pillai and Salgado (1994). Table-2 shows the key parameters used in the performance analyses. For the design earthquake (M6.5, PGA=0.12g) considered, both the Lab.method and Seed's method predict a significant extent of liquefaction of the foundation soils (unit-3c) under the downstream slope in the right half of the dam. However, because of the large confining stresses present at Duncan Dam, the Lab.method indicates significantly higher residual strengths than those predicted by Seed's chart. Consequently, the Lab.method predicts satisfactory performance with respect to post-liquefaction deformations and stability of the dam. On the other hand, Seed's method predicts unstable slopes and a flow slide causing large deformations

TABLE 2

TABLE OF KEY PARAMETERS
Lab Method and Seed's Method

Performance Analysis	Lab Method	Seed's Method
Triggering Analysis/ Liquefaction Resistance	CRR_1 = 0.14 K_α < 1.0 (as per lab tests) K_α = 1.0	CRR_1 = 0.12 K_α < 1.0 (as per lab tests) K_α = 1.0
Slope Stability Analysis/ Residual Strength of Liquefied Zone	S_{ur} = 0.12 σ_{vo}'	S_{ur} = f $(N_1)_{60}$ or = (.12 P_a + .03σ_{vo}')
Deformation Analysis/ Post Liquefaction Shear Modulus	For α < 0.1 G_L = .21 σ_{vo}'/0.25 For α > 0.1 G_L = .21 σ_{vo}'/0.025	For α < 0.1 G_L = (.12 P_a + .03σ_{vo}')/0.25 For α >0.1 G_L = (.12P_a + .03σ_{vo}')/0.025

leading to a failure of the dam. Due to the empiricism in the indirect method developed by Dr.H.B.Seed and his co-workers, and the required extrapolations beyond the empiricism, it was concluded that the direct method provided an improved understanding of the dam behaviour during seismic loading. Thus it was concluded that the risk of a flow slide occurring at Duncan Dam is negligible for the maximum design earthquake considered and therefore no retrofit measures for the dam would be required.

CONCLUSIONS

The field and laboratory investigations that were carried out at Duncan Dam were extensive and represent some recent advances in liquefaction assessment of foundation soils beneath large civil structures. It has been possible to successfully freeze insitu a preselected zone of foundation sands at Duncan Dam and obtain undisturbed sand samples. Standard investigation techniques coupled with advanced geophysical testing, insitu and laboratory testing has provided corroboration of the high quality of the frozen samples.

The laboratory testing program on unit-3c sand has provided an understanding of some fundamental shear behavioural aspects such as:

1. The stress-path or loading mode dependency of both monotonic and cyclic behaviour of sand.
2. The influence of confining stress on liquefaction resistance and the significant difference of the K_σ-factor for the Duncan Dam from the commonly used K_σ based on Seed and Harder (1990).
3. The influence of static bias on liquefaction resistance and a rational basis for the application of K_α which is dependent on the stress-path and initial state of the soil.
4. The influence of initial static bias on the post-cyclic stress-strain response and the stiffness of the liquefied sand.
5. The relationship of initial confining stress on the residual strength (S_{ur}/σ_{vo}' = 0.21).

Application of these factors to seismic assessment of Duncan Dam has resulted in the conclusion that post-liquefaction deformations will be tolerable and no remedial work is required for the maximum design earthquake. Whereas the simpler and more conventional assessment using Seed's method predicted a flow-slide and remedial requirements.

ACKNOWLEDGEMENTS

The authors wish to thank BC Hydro for permission to publish this paper. Also we thank Dr.Yogi Vaid for his interest and supervision of the laboratory testing. The opinions expressed in this paper are those of the authors and do not necessarily represent those of any other individual or organization.

REFERENCES

GIBBS, H.J. and HOLTZ, W.G., 1957. Research on Determining the Density of Sands by Spoon Penetration Testing. Proceedings, 4th Int.Conf.on Soil Mechanics and Foundation Engineering, London, Vol.1, pp 35-39.

ISHIHARA, K. 1993. Liquefaction and flow failure during earthquakes. Geotechnique Vol.43, No. 3, 351 - 415.

LIAO, S.C. and WHITMAN, R.V., 1986. Overburden Correction Factors for SPT in Sand. Journal of Geotechnical Engineering Division, ASCE, Vol.112, No.3., pp 373 -377.

PILLAI, V.S., 1991. Liquefaction analysis of sands: Some interpretations of Seed's K_α (sloping ground) and K_σ (depth) correction factors using steady state concept. Proceedings: Second International Conference on Recent Advances in Geotechnical Earthquake Engineering and Soil Dynamics. March 11-15, St. Louis, Missouri, pp 579-587.

PILLAI, V.S. and BYRNE, P.M., 1994. Effect of Overburden Stress on Liquefaction Resistance of Sand. Canadian Geotechnical Journal, Vol.31, No.1, pp 53-60.

PILLAI, V.S., and SALGADO, F.M., 1994 Post-Liquefaction Stability and Deformation Analysis of Duncan Dam, (in press) Canadian Geotechnical Journal, Vol.31, No.6 (December, 1994).

PILLAI, V.S., and STEWART, R.A. 1994 Evaluation of Liquefaction Potential of Foundation Soils of Duncan Dam, (in press) Canadian Geotechnical Journal, Vol.31, No.6, (December,1994).

PLEWES, H.D., PILLAI,V.S., MORGAN,M.R. and KILPATRICK,B.L.,1994 In situ Sampling, Density Measurements and Testing of Foundation Soils at Duncan Dam.(in press) Canadian Geotechnical Journal, Vol.31, No.6 (December, 1994).

PLEWES,H.D., McROBERTS, E.C., CHAN, W.K. 1988 Downhole Nuclear Density Logging in Sand Tailings. ASCE Specialty Conference on Hydraulic Fill Structures, Fort Collins, Colorado, pp 290-309.

SEGO, D.S., ROBERTSON, P.K., SASITHARAN, S., KILPATRICK, B.L. and PILLAI, V.S., 1994. Ground Freezing and Sampling of Foundation Soils at Duncan Dam, (in press) Canadian Geotechnical Journal, Vol.31, No.6 (December,1994).

SEED, H.B., and de ALBA, P, 1984. Use of SPT and CPT Tests for Evaluating the Liquefaction Resistance of Sands, INSITU 86, ASCE Specialty Conference on Use of Insitu Testing in Geotechnical Engineering, Geot.Spec.Publ.No.6,ASCE, pp 281-302

Seed and Idriss, 1982. Ground Motions and Soil Liquefaction Potential During Earthquakes. monograph series. EERI, Berkeley, California.

SEED, H.B., TOKIMATSU, K., HARDER, L.F. and CHUNG, R.M., 1984. The Influence of SPT Procedures in Evaluating Soil Liquefaction Resistance. EERC-88-04, Univ. of California, Berkeley, California.

SEED, R.B. and HARDER, L.F., 1990. SPT-Based Analysis of Cyclic Pore Pressure Generation and Undrained Residual Strength. H. Bolton Seed Memorial Symposium Proceedings, May 1990 Vol. 2, 351-376.

Skempton, A.W., 1986. Standard Penetration Test Procedures and the Effects in Sands of Overburden Pressure, Relative Density, Particle Size, Ageing and Overconsolidation. Geotechnique 36, No.3, pp. 425-447.